

Anti-thrombogenicity by Layer-by-Layer Self-assembled Polyelectrolyte Film

Seimei Shiratori and Tomomi Matsuda

Graduate School of Science and Technology, Keio University, Kohoku-ku, Hiyoshi 3-14-1, Japan
e-mail: shiratori@appi.keio.ac.jp

Abstract. Anti-thrombogenic films with high durability were fabricated in a wet process. Anti-thrombogenicity was achieved with polyelectrolyte multilayer thin film prepared from poly(vinyl alcohol)-poly(acrylic acid)(PVA-PAA) blends, deposited in alternate layers with poly(allylamine hydrochloride) (PAH). Film durability, assessed by abrasion resistance and water resistance, was enhanced by forming crosslinks via amide bonds induced by heat treatment of the film. The film was found to be resistant to protein adsorption, as measured by the amount of fibrinogen adsorbed from an aqueous solution. Anti-thrombogenic efficacy was assessed in ex vivo experiments by the ability of stainless steel mesh, coated with the polyelectrolyte and inserted into a pig blood vessel, to inhibit thrombus formation. Mesh coated with the polyelectrolyte did not reduce blood flow over a period of 15 minutes, whereas with uncoated mesh blood flow stopped within 6 minutes because of blood vessel blockage by thrombus formation.

1 Introduction

The use of medical equipment such as endoscopes and catheters inside the body has increased. However, medical equipment is recognized as foreign by the human body, when it comes into contact with blood, causing formation of a thrombus (blood clot) on the surface of the equipment. Consequently, the performance of medical equipment may be reduced, and blockage of blood vessels may result. For those reasons, there is a need to control thrombus formation on medical equipment.

Only a few findings have been reported regarding the effect of surface morphology on small proteins such as lysozyme and cytochrome^{1, 2}; the majority of reports have focused on the effects of surface chemistry^{3, 4, 5, 6}. The surfaces can be categorized into four main types, namely heparinized or biological surfaces⁷, electrically charged surfaces⁸, inert surfaces^{9, 10} and solution-perfused surfaces¹¹. Films with these surface properties have been successfully fabricated using heparin, modified collagen, carbons, polyethylene glycol (PEG)^{12, 13}. However, most of the protein resistance data for these films have not been evaluated in vivo, and the fabrication methods for the films required complex procedures or expensive conditions such as high vacuum. As one of easy and low-cost fabrication technique, layer-by-layer self-assembly (LbL)¹⁴ method is well-known. By using this LbL method, various applications have been developed such as biomimetic membrane for biosensors¹⁵, field effect transistor¹⁶, nano-hollow templates for drug delivery systems¹⁷, and other nanostructured applications¹⁷.

In this study, the effect of film surface charge (zeta potential) as well as surface morphology was investigated using the self-assembly Layer-by-Layer method to fabricate highly antithrombogenic films. It was confirmed that the thin film had high anti-thrombogenicity in vivo. In addition, the film durability was drastically improved by creating crosslinks via amide bonding in the film.

2 Materials & Methods

2.1 Materials. Poly(diallyldimethyl ammonium chloride) (PDDA, Mw 400-500 kg/mol, 20 wt% aqueous solution; 100 mM, with no pH adjustment), poly(allylamine hydrochloride) (PAH, Mw ~70 kg/mol; 100 mM, pH7.5), and poly(acrylic acid) (PAA, molecular weight ~100 kg/mol, 35 wt% aqueous solution; 20 mM, pH3.5). Poly(vinyl alcohol) (PVA, molecular weight ~66 kg/mol; 1 mg/ml, pH3.5) were used as materials. All polyelectrolyte dipping solutions were made from ultrapure water, and the pH was adjusted with NaOH^{18, 19}. Glass slides were cleaned in KOH solution for 2 min, followed by thorough rinsing with water and drying.

2.2 Polyelectrolyte Blend Multilayer Film Buildup. Anionic polyelectrolyte layers were deposited from a PVA-PAA solution blend. Cationic polyelectrolyte layers were deposited from a solution of PDDA or PAH. Glass and silicon substrates were alternately immersed in anionic polyelectrolyte blend solutions and PDDA or PAH solutions for 15 min, and rinsed with water (2 min, 1 min, 1 min) after deposition of each layer. The films were dried

after multilayer assembly in a gentle stream of nitrogen. The multilayer films are represented as (PDDA or PAH/(PVA+PAA))_n, where 'n' is the number of bilayers and 'PVA+PAA' refers to the solution blend of PVA-PAA. Crosslinking was carried out by inducing ester bonding in PDDA/(PVA+PAA) film and amide bonding in PAH/(PVA+PAA) film, by heating.

2.3 Durability testing.

Abrasion tests were carried out using an abrasion machine in cloth-on-plate contact configuration, with a 100 g/cm² load. A piece of the cloth was moved across the sample at 500 mm/min over a distance of 30 mm by 100 round trips. Water resistance tests were carried out by immersion of samples in water for 180 min, then the films were dried. The morphologies of the films before and after abrasion testing were observed using FE-SEM.

2.4 Protein adsorption. Protein adsorption on polyelectrolyte blend films was examined via FT-IR. Silicon wafers coated with the polyelectrolyte blend films were immersed for 20 min in phosphate buffered saline (PBS) containing 0.5 mg/ml fibrinogen, followed by rinsing with PBS (1 min) and N₂ drying^{20, 21, 22, 23}. Fibrinogen was identified by the amide C-N-H vibrational bands of amide groups (CO-NH). Fibrinogen is a protein produced by the liver. This protein stop bleeding by helping blood clots to form.

2.5 Anti-thrombogenicity. Evaluation of anti-thrombogenicity was carried out on animals. Stainless steel meshes coated with polyelectrolyte were inserted into a pig's blood vessel. The change of blood flow volume was measured for 15 min. Blood flow stops because of formation of a thrombus when there is no anti-thrombogenicity, whereas a thrombus is not formed and blood flow is maintained when there is an anti-thrombogenic effect.

3 Results and Discussions

3.1. Surface zeta potential of film surfaces

Fig.1 shows the zeta potentials of various film surfaces before and after contact with fibrinogen.

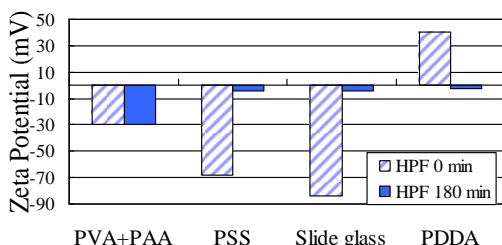


Fig.1. Surface zeta potentials of various films before and after exposure to fibrinogen.

Before contact with fibrinogen, films with anionic outermost surfaces (PVA+PAA, PSS, slide glass) were observed to have a negative surface charge, while the cationic PDDA surface was observed to have a positive charge. The only film with little change before and after exposure to fibrinogen was the film with an outermost surface layer of anionic PVA+PAA. As presumed, anionic surfaces (PVA+PAA, PSS, slide glass substrate) exhibited

an initial negative zeta potential, while the cationic PDDA film surface was positively charged (Fig.1). After exposure to fibrinogen for 180 min, the cationic PDDA film resulted in adsorbing more fibrinogen than the negatively charged surfaces. This is most likely due to the attractive forces between the positively charged PDDA surface and the negatively charged fibrinogen. Also, the results from the zeta potential measurements showed that the PVA+PAA film surface showed the highest resistance to fibrinogen adsorption. This observation suggested other factors to be affecting the fibrinogen adsorption.

3.2. Transparency of film surfaces

Fig.2 shows the transmittance of various film surfaces after contact with fibrinogen for 180 min.

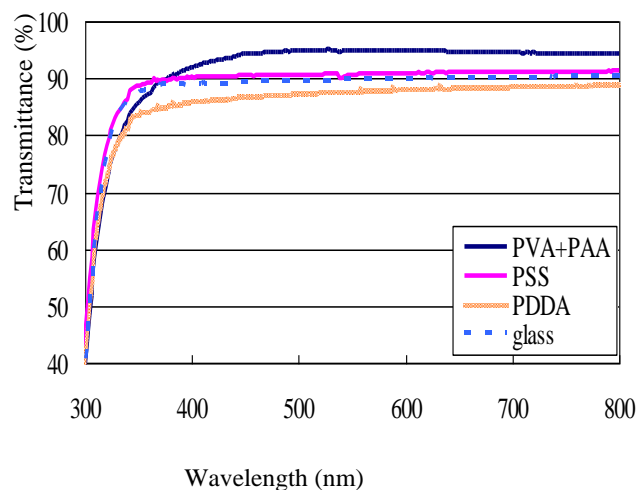


Fig.2. Transmittance of various films after 180 min exposure to fibrinogen.

The mixed solution of anionic PVA and PAA showed the highest transparency, while the film with an outermost surface layer of cationic PDDA resulted in having the lowest transparency.

The average transmittance decrease for each film was about 1% for the mixed solution of PVA and PAA, 5% for the PSS and glass substrate control, and 8% for the PDDA film within the wavelength range of visible light. For each experiment the error was less than 1%.

The amount of fibrinogen adsorbed onto the surface of each film was compared with the change in transmittance. Fig.2 shows that the film with an outermost surface layer of PVA+PAA resulted in adsorbing the least amount of fibrinogen, while the positively charged PDDA film surface adsorbed the largest amount of fibrinogen. Both of the PSS and slide glass substrate adsorbed fibrinogen. This supports the conclusion that the difference in zeta potential change shown in Fig.1 corresponds with the amount of fibrinogen adsorbed onto the films. In these experiments, it was found that the best film to avoid the adsorption of fibrinogen was PVA+PAA.

Therefore, we utilize the PVA +PAA composite layer as the anionic layer of layer-by-layer deposition. Since we have found that the PVA +PAA composite anionic solution and PAH cationic solution is good combination for the layer-by-layer deposition, we decide to fabricate PAH/(PVA+PAA) films. Number of the deposition cycle was

10 in this experiment and we describe as $(\text{PAH}/(\text{PVA}+\text{PAA}))_{10}$.

3.3. Abrasion test of self-assembled structure

Fig. 3 displays polyelectrolyte multilayer morphologies as imaged by FE-SEM. The surface structures of non-crosslinked $\text{PAH}/(\text{PVA}+\text{PAA})$ films were removed in the abrasion test, while the structures of crosslinked $\text{PAH}/(\text{PVA}+\text{PAA})$ films were maintained.

For the abrasion resistance of $\text{PAH}/(\text{PVA}+\text{PAA})$ film was improved considerably by heat treatment induced amide bonding.

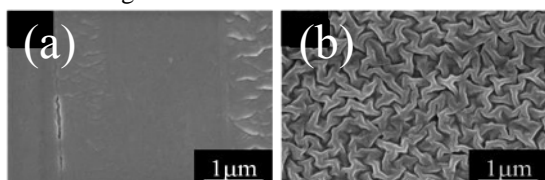


Fig. 3. SEM surface topography images ($\times 25000$) of polyelectrolyte films after abrasion. (a) non-crosslinked, and (b) crosslinked $(\text{PAH}/(\text{PVA}+\text{PAA}))_{10}$ films.

3.4. Water resistance.

Fig. 4 displays polyelectrolyte multilayer film morphologies, after immersion of the films in water, as imaged by FE-SEM. The surface structure of non-crosslinked $\text{PAH}/(\text{PVA}+\text{PAA})$ disappeared on rinsing, whereas the structure of crosslinked $\text{PAH}/(\text{PVA}+\text{PAA})$ films remained after contact with water.

The longer that non-crosslinked $\text{PAH}/(\text{PVA}+\text{PAA})$ films were in contact with water, the greater the extent to which the surface structure disappeared: the structure began to collapse in 30 min and disappeared after 180 min. For the $\text{PAH}/(\text{PVA}+\text{PAA})$ films that had been crosslinked, the surface structure remained after 180 min immersion in water. The improvement of water resistance of $\text{PAH}/(\text{PVA}+\text{PAA})$ films is attributed to heat treatment induced ester bonding and amide bonding, respectively. For $\text{PAH}/(\text{PVA}+\text{PAA})$ films, PVA intertwines with PAA, thus the PVA is not easily dissolved in water. A proportion of the hydrophilic groups were lost because the amide bonds were formed (Fig. 5)²⁴, and the water resistance improved.

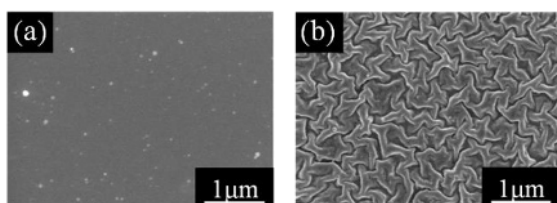


Fig. 4. SEM surface topography images ($\times 25000$) of polyelectrolyte films after immersion in water. (a) non-crosslinked, and (b) crosslinked $(\text{PAH}/(\text{PVA}+\text{PAA}))_{10}$ films.

3.5. Biocompatibility of the films

Fig.5 shows FT-IR spectrum of fibrinogen solution. Fibrinogen was identified by the amide 1 and 2 bands of

amide groups. If fibrinogen adsorbs on the surface, then the amide 1 and 2 bands appear. Fig.6 shows FT-IR spectra of the hierarchical structure film before and after being in contact with fibrinogen solution. The FT-IR data clearly demonstrate that fibrinogen was not adsorbed on the hierarchical structure film.

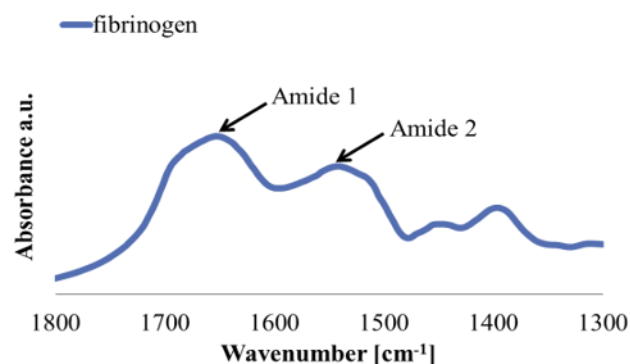


Fig.5 FT-IR spectrum of fibrinogen solution.

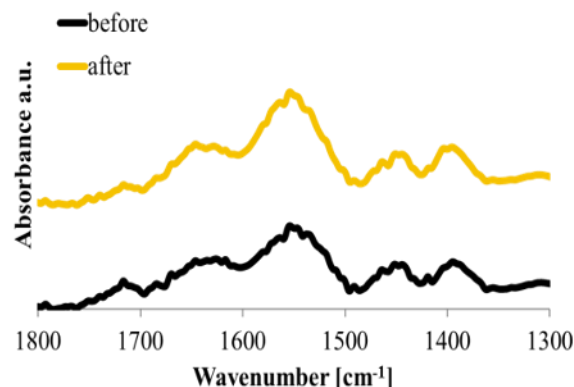


Fig.6 FT-IR spectra of the new film before and after being in contact with fibrinogen solution.

3.6. Anti-thrombogenicity. Fig. 7 shows the time course of the blood flow volume in the blood vessel with polyelectrolyte multilayer-coated stainless steel mesh inserted. Schematic images of thrombus formation in an animal blood vessel is shown in Fig.8 to clarify the results shown in Fig.7. If the stainless steel mesh is not biocompatible, a thrombus is formed on the surface, and the blood flow volume gradually decreases. However, if the coated mesh is biocompatible, a thrombus is not formed on the surface and the blood flow is maintained. In the case of the “Control” (an uncoated stainless steel mesh) the blood flow volume decreased rapidly because of thrombus formation. For the mesh coated with non-crosslinked PDDA/ $(\text{PVA}+\text{PAA})$ the blood flow volume was maintained for at least 15 min. However, the crosslinked PDDA/ $(\text{PVA}+\text{PAA})$ coating caused the blood flow volume to cease after 11 min. With mesh coated with either crosslinked or non-crosslinked $\text{PAH}/(\text{PVA}+\text{PAA})$ blood flow volume was maintained for 15 min.

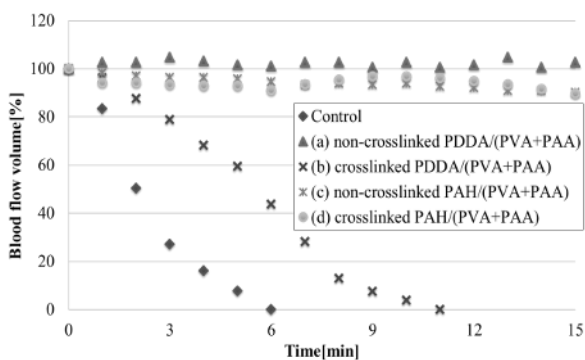


Fig. 7. Anti-thrombogenicity of (a-d) films inserted in an animal blood vessel.

(a) non-crosslinked, and (b) crosslinked (PDDA/(PVA+PAA))₁₀;
(c) non-crosslinked, and (d) crosslinked (PAH/(PVA+PAA))₁₀.

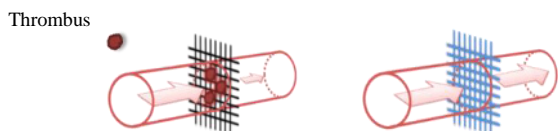


Fig. 8. Schematic images of thrombus formation in an animal blood vessel.

The compatibility between PVA and PAA is high; hence PVA stays in the anionic layer by being intertwined with PAA, so that most of the OH groups of PVA exist freely in the anion layer. Consequently, anti-thrombogenicity was achieved through the OH groups²⁵⁻²⁹.

For the PAH/PAA films, the NH₃⁺ groups of PAH and COO⁻ groups of PAA interact by electrostatic attraction, and the film does not show anti-thrombogenicity. It can be concluded that anti-thrombogenicity was achieved by the accessible OH groups. Moreover, when PAH/(PVA+PAA) films were heat treated, amide bonds were formed between NH₃⁺ groups of PAH and COO⁻ groups of PAA²⁹. Consequently, most of the OH groups of PVA exist freely in the anion layer, as for non-crosslinked PAH/(PVA+PAA) film, and the crosslinked PAH/(PVA+PAA) film retained anti-thrombogenicity because hydrophilic OH groups were accessible in the anion layer.

Thus, non-crosslinked PAH/(PVA+PAA), crosslinked PAH/(PVA+PAA) and non-crosslinked PDDA / (PVA+PAA) have more free hydroxyl groups compared with crosslinked PDDA/(PVA+PAA). And, non-crosslinked PAH/(PVA+PAA) film, crosslinked PAH/(PVA+PAA) film and non-crosslinked PDDA/(PVA+PAA) film show anti-thrombogenicity.

As for effect of surface morphologies, it is possible that surface morphologies may shed protein and inhibit the formation of thrombus. If the surface morphologies contribute to the anti-thrombogenicity, all four types of film should have protein resistance and anti-thrombogenicity. However, the result was different. Consequently, we concluded that an important factor concerning protein resistance and anti-thrombogenicity is not the surface morphologies but the surface functional groups: the free hydroxyl group.

4 Conclusions

Anti-thrombogenicity was achieved with polyelectrolyte multilayer thin film prepared from poly(vinyl alcohol)-

poly(acrylic acid)(PVA-PAA) blends, deposited in alternate layers with poly(allylamine hydrochloride) (PAH). The water and abrasion resistance of PAH/(PVA+PAA) films was improved by thermal treatment, which led to amide bonding, hence crosslinking, in PAH/(PVA+PAA). This covalent bonding improved the durability of the films. The amide bonding between the acid groups of PAA and the amine groups of PAH did not influence the anti-thrombogenicity because free hydroxyl groups of PVA contributed to maintenance of anti-thrombogenicity. Thus PAH/(PVA+PAA) film after heat treatment had high durability, high protein resistance, and anti-thrombogenicity. We consider that this material should be useful as an anti-thrombogenic surface coating for catheters, artificial blood vessels, and so on.

References

1. Vertegal, A. A.; Siegel, R. W.; Dordick, J. S. *Langmuir* **2004**, *20*, 6800-6807
2. Tain, M.; Lee, W. K.; Bothwell, M. K.; McGuire, J. J. *Colloid Interface Sci.* **1988**, *200*, 146-154
3. Keselowsky, B. G.; Collard, D. M.; Garcia, A. J. *Biomaterials* **2004**, *25*, 5947-5954
4. Roach, P.; Farrar, D.; Perry, C. C. *J. Am. Chem. Soc.* **2005**, *127*, 8168-8173
5. Hobora, D.; Imabayashi, S. I.; Kakiuchi, T. *Nano Lett.* **2002**, *2*, 1021-1025
6. Hasebe, T.; Ishimaru, T.; Kamijo, A.; Yoshimoto, Y.; Yoshimura, Y.; Yohena, S.; Kodama, H.; Hotta, A.; Takahashi, K.; Suzuki, T. *Diamond & Related Materials* **2007**, *16*, 1343-1348
7. Ferguson, A. B.; Akahoshi, Y.; Laing, P. G.; Hodge, E. S. *J. Bone Jt. Surg.* **1962**, *44A*, 323-336
8. Hoffman, A. S. *Radiat. Phys. Chem.* **1977**, *9*, 207-219
9. Young, C. D.; Wu, J. R.; Tsou, T. L. *Journal of membrane science* **1988**, *146*, 83-93
10. Karadag, E.; Saraydin, D.; Cetinkaya, S.; Guyen, O. *Biomaterials* **1996**, *17*, 67-70
11. Clarke, D. R.; Park, J. B. *Biomaterials* **1981**, *2*, 9-13
12. Kingshott, P.; Thissen, H.; Griesser, H. J. *Biomaterials* **2002**, *23*, 2043-2056
13. Xu, Z. L.; Qusay, F. A. *Journal of Applied Polymer Science* **2004**, *91*, 3398-3407
14. G. Decher et al., *Thin Solid Films* **1992**, 210/211, 831.
15. Tang, Z.; Wang, Y.; Podiadlo.; Kotov, N. A. *Adv. Mater.* **2006**, *18*, 3203-3224
16. Ariga, K.; Hill, J. P.; Ji, Q. *Phys. Chem. Chem. Phys.* **2007**, *9*, 2319-2340
17. Wang, Yajun.; Angelatos, A. S.; Caruso, F. *Chem. Mater.* **2008**, *20*, 848-858
18. Shiratori, S. S.; Rubner, M. F. *Macromolecules* **2000**, *33*, 4213-4219
19. Yoo, D.; Shiratori, S. S.; Rubner, M. F. *Macromolecules* **1988**, *31*, 4309-4318
20. Mendelsohn, J. D.; Yang, S. Y.; Hiller, J. A.; Hochbaum, A. I.; Rubner, M. F. *Biomacromolecules* **2003**, *4*, 96-106
21. Quinn, A.; Tjipto, E.; Yu, A.; Gengenbach, T. R.; Caruso, F. *Langmuir* **2007**, *23*, 4944-4949
22. Yang, S. Y.; Mendelsohn, J. D.; Rubner, M. F. *Biomacromolecules* **2003**, *4*, 987-994
23. Tristan, F.; Palestino, G.; Menchaca, J. L.; Perez, E.; Atmani, H.; Cuisinier, F.; Ladam, G. *Biomacromolecules* **2009**, *10*, 2275-83
24. Arndt, K. F.; Richter, A.; Ludwig, S.; Zimmermann, J.; Kressler, J.; Kuckling, D.; Adler, H. J. *Acta Polym.* **1999**, *50*, 383-390
25. Quinn, A.; Such, G. K.; Quinn, J. F.; Caruso, F. *Adv. Funct. Mater* **2008**, *18*, 17-26
26. Ma, C.; Hou, Y.; Liu, S.; Zhang, G. *Langmuir* **2009**, *25*, 9467-9472
27. Choi, J.; Rubner, M. F. *Macromolecules* **2005**, *38*, 116-124
28. Ikada, Y.; *Adv. Polym. Sci.* **1983**, *57*, 103-140
29. M. Matsuda, S. Shiratori, *Langmuir*, *27*, 4271(2011)